

C.P. No. 299
(16,932)
A.R.C. Technical Report

C.P. No. 299
(16,932)
A.R.C. Technical Report



MINISTRY OF SUPPLY

AERONAUTICAL RESEARCH COUNCIL
CURRENT PAPERS

Transient Thermal Stress in a
Flat Plate Due to Non-Uniform
Heat Transfer Across One Surface

By

N. S. Heaps, B.Sc.

LONDON: HER MAJESTY'S STATIONERY OFFICE

1956

FOUR SHILLINGS NET

U.D.C. No. 539.319 : 533.6.011.6

Report No. Structures 164

April, 1954

ROYAL AIRCRAFT ESTABLISHMENT

Transient Thermal Stress in a Flat Plate Due to
Non-Uniform Heat Transfer Across One Surface

by

H. S. Heaps, B.Sc.

SUMMARY

Transient thermal stresses are determined theoretically for a long rectangular plate when subjected to a sudden change in temperature on its top surface. On this surface a heat transfer coefficient is postulated which varies inversely as the square of the distance from one of the longitudinal edges. The solution in terms of Bessel Functions has application to the aerodynamic heating of the wings of an aircraft when suddenly accelerated to a high supersonic speed.

LIST OF CONTENTS

	<u>Page</u>
1 Introduction	4
2 Statement of the problem	4
3 Basic assumptions	5
4 Solution of the problem	5
4.1 The equation of heat conduction	5
4.2 The temperature distribution	6
4.3 Thermal stresses	7
4.4 Non-dimensional parameters	8
5 Numerical examples, relevant to cases of aerodynamic heating in supersonic flight	8
5.1 Numerical results	9
6 Conclusions	10
List of symbols	11
References	13

LIST OF APPENDICES

	<u>Appendix</u>
Determination of the coefficients, A_n	I
Derivation of expressions for	
$I(n, \frac{1}{2}, p), F = \frac{2j+1}{2} (j = 1, 2, \dots, 6)$	II
Heat transfer data for a flat plate	III
Numerical analysis	IV

LIST OF TABLES

	<u>Table</u>
Data for the numerical examples	1

LIST OF ILLUSTRATIONS

	<u>Figure</u>
The plate, showing notation.	1(a,b)
Aerodynamic heating of the plate, showing the direction of the supersonic air stream over the top surface.	2(a,b)
Heat transfer coefficients.	3
Temperature and stress distributions in the plate at various times for	
$\frac{1}{10^3} \cdot \frac{hL^2}{ks} = \frac{0.012}{\xi^2} + 0.1774.$	4(a,b)
Temperature and stress distributions in the plate at various times for	
$\frac{1}{10^3} \cdot \frac{hL^2}{ks} = \frac{0.042}{\xi^2} + 2.306.$	5(a,b)
Maximum stress in the plate at various times.	6

1 Introduction

The problem solved in this paper is that of a long rectangular plate at uniform temperature which is suddenly exposed to a higher temperature in the immediate proximity of its top surface.* On the exposed surface a heat transfer coefficient is postulated which varies inversely as the square of the distance from one of the longitudinal edges. A state of no heat transfer is postulated for the edges of the plate. Under these conditions there is a non-uniform transference of heat to the plate, giving rise to transient temperature gradients and thermal stresses within the plate. The temperatures and stresses are derived theoretically with certain simplifying assumptions.

The solution in terms of Bessel Functions is then used to estimate transient thermal stresses induced in an aircraft wing when suddenly acquiring a high supersonic velocity. Hoff¹ calculated the stresses in a spar web by assuming a uniform heat transfer coefficient on the wing surfaces, and this work was later extended by Parkes². The stresses now considered are those in a wing skin due to chordwise variation of heat transfer coefficient on the wing surfaces described by Kaye³. The law of variation of heat transfer coefficient postulated was chosen to give a convenient analytical solution of the heat conduction equation, and to be at the same time a reasonable approximation to the actual variation of heat transfer coefficient in flight.

2 Statement of the problem

Diagrams of the plate under consideration are shown in Fig. 1[(a),(b)]. O is a point on one of the longitudinal edges and x, y are distances measured from O in lateral and longitudinal directions, respectively. The width of the plate is denoted by L, and its thickness by s. The thermal conductivity of the material of the plate is denoted by k.

Initially the plate and its surroundings are at a uniform temperature θ_0 . The temperature in the immediate proximity of the top surface then changes instantaneously to a constant value θ_1 . Heat is subsequently transferred across the surface at a rate governed by a heat transfer coefficient, $h(x)$, which is postulated in the form:

$$\frac{L^2 \cdot h(x)}{ks} = \frac{p^2 - \frac{1}{4}}{(x/L)^2} + q, \quad (1)$$

where p and q are arbitrary non-dimensional constants such that $p > \frac{1}{2}$, $q > 0$. A state of no heat transfer is postulated across the other surfaces of the plate.

Under these conditions transient temperature gradients and hence transient thermal stresses develop in the plate, heat conduction taking place until the temperature throughout the plate is θ_1 . Since the thickness of the plate is small in comparison with its lateral and longitudinal dimensions the temperature at any position on the plate is assumed constant through the thickness and is denoted by $\theta(x,t)$. On this assumption it is required to solve the problem of linear heat conduction parallel to Ox, thus to determine the temperature distribution $\theta(x,t)$ and thence the thermal stresses in the plate.

In determining the thermal stresses it is postulated that the plate is free from applied forces. Other stresses due to applied forces may be determined separately, the total stresses being obtained by superposition.

* The theory is equally applicable to a cooled plate.

3 Basic assumptions

- (i) At any position on the plate the temperature is constant through the thickness.
- (ii) The stress system in the plate is entirely longitudinal and may, therefore, be determined on the basis that lateral cross-sections remain plane.
- (iii) Stress-strain relations are linear.
- (iv) Young's modulus and the coefficient of linear expansion do not vary with temperature.
- (v) Elastic displacements are small.
- (vi) Buckling does not occur.

4 Solution of the problem

In this section the problem is analysed and solved, mathematical details being given in Appendices I and II. The equation of linear heat conduction is derived in para. 4.1. Solving this equation, putting in the appropriate boundary and initial conditions, the temperature distribution is deduced in para. 4.2. An expression for the subsequent evaluation of the thermal stresses is obtained in para. 4.3. Finally, the non-dimensional parameters of the problem are summarised in para. 4.4, a preliminary mention being made of some numerical plots.

4.1 The equation of heat conduction

The conditions of heat flow for an element of the plate between x and $x + dx$, of unit length, and bounded by the top and bottom flat surfaces, are now considered (see Fig.1). Between x and $x + dx$, heat is being transferred across the top surface at a rate

$$dQ = (\theta_1 - \theta) h(x) dx . \quad (2)$$

At x , in the plate, heat is being conducted in the direction of positive x at a rate

$$Q_x = - ks \frac{\partial \theta}{\partial x} , \quad (3)$$

while at $x + dx$, the value is

$$Q_x + dQ_x = - ks \left(\frac{\partial \theta}{\partial x} + \frac{\partial^2 \theta}{\partial x^2} dx \right) . \quad (4)$$

The element $(x, x + dx)$ is, therefore, gaining heat at a rate

$$dQ - dQ_x = \left[(\theta_1 - \theta) h(x) + ks \frac{\partial^2 \theta}{\partial x^2} \right] dx , \quad (5)$$

which causes its temperature to rise at a rate

$$\frac{\partial \theta}{\partial t} = \frac{dq - dq_x}{\rho c s dx} \quad (6)$$

Combining equations (5) and (6) gives the equation of heat conduction

$$\frac{\partial \theta}{\partial t} = k \frac{\partial^2 \theta}{\partial x^2} - \frac{h(x)}{\rho c s} (\theta - \theta_1) \quad (7)$$

Introducing a non-dimensional parameter $\xi = \frac{x}{L}$, it may be shown that a solution of equation (7) is

$$\theta - \theta_1 = X(\xi) e^{-\left(\beta^2 + q\right) \frac{kt}{L^2}} \quad (8)$$

where X satisfies the equation

$$\frac{d^2 X}{d\xi^2} + \left(\beta^2 + q - \frac{L^2 h(\xi L)}{ks} \right) X = 0, \quad (9)$$

and β is a constant.

For the variation of the heat transfer coefficient, h , given by equation (1), equation (9) becomes

$$\frac{d^2 X}{d\xi^2} + \left(\beta^2 - \frac{4p^2 - 1}{4\xi^2} \right) X = 0, \quad (10)$$

which is Bessel's Equation of order p , expressed in the "normal" form.

4.2 The temperature distribution

A solution of equation (10) which satisfies one boundary condition of the problem - the condition of no heat flow $\left(\frac{\partial \theta}{\partial x} = 0 \right)$ at $x = 0$, is

$$X = A \xi^{\frac{1}{2}} J_p(\beta \xi), \quad (11)$$

where $J_p(\beta \xi)$ is a Bessel Function of the First Kind, and A is an arbitrary constant. Assuming this form of solution, the other condition of no heat flow at $x = L$ leads to the equation

$$\left(\frac{1}{2} - p \right) J_p(\beta) + \beta J_{p-1}(\beta) = 0, \quad (12)$$

the roots of which are denoted, in ascending order of magnitude, by $\beta_n (n = 1, 2, \dots)$.

It now follows from equations (8) and (11) that a solution of the equation of heat conduction satisfying the boundary conditions of the problem is

$$\theta - \theta_1 = \sum_{n=1}^{\infty} A_n \xi^{\frac{1}{2}} J_p(\beta_n \xi) e^{- (\beta_n^2 + q) \frac{\kappa t}{L^2}} \quad (13)$$

The constant coefficients A_n are determined, in Appendix I, to satisfy the initial condition, $\theta = \theta_0$ at $t = 0$. It is subsequently found that

$$\frac{\theta - \theta_1}{\theta_0 - \theta_1} = \sum_{n=1}^{\infty} \frac{2(\beta_n \xi)^{\frac{1}{2}} J_p(\beta_n \xi) I(n, \frac{1}{2}, p)}{(\frac{1}{2} - p^2 + \beta_n^2) [J_p(\beta_n)]^2} e^{- (\beta_n^2 + q) \frac{\kappa t}{L^2}} \quad (14)$$

where

$$I(n, \frac{1}{2}, p) = \int_0^{\beta_n} \eta^{\frac{1}{2}} J_p(\eta) d\eta \quad (15)$$

$\frac{\theta - \theta_1}{\theta_0 - \theta_1}$, determined from equation (14), is a non-dimensional parameter giving the temperature distribution, $\theta(x,t)$, in the plate.

For $p = \frac{2j+1}{2}$ ($j = 1, 2, \dots, 6$), expressions are derived in Appendix II which give $I(n, \frac{1}{2}, p)$ in terms of powers of β_n , $J_p(\beta_n)$, $\sin \beta_n$, and the sine integral $S_{\frac{1}{2}}(\beta_n)$. Tables of $J_p(\eta)$ and $S_{\frac{1}{2}}(\eta)$ are available for numerical work^{9,10,11,12,13,14}.

4.3 Thermal stresses

It is assumed that the stress system in the plate is entirely longitudinal. It may, therefore, be determined on the basis that lateral cross-sections remain plane, from which it follows that

$$f = E(-\alpha\theta + e_1 + a_1 x) \quad (16)$$

where E denotes Young's modulus, α denotes the coefficient of linear expansion, and e_1, a_1 , are constants.

The plate is considered to be free from applied forces and, therefore,

$$\left. \begin{aligned} \int_0^L f dx &= 0, \\ \int_0^L x f dx &= 0, \end{aligned} \right\} \quad (17)$$

which, when combined with equation (16), yield expressions for e_1 and a_1 . Substituting these expressions back into equation (16) gives

$$\frac{f}{E\alpha(\theta_1 - \theta_0)} = \Omega - 2(2 - 3\xi) \int_0^1 \Omega d\xi + 6(1 - 2\xi) \int_0^1 \xi \Omega d\xi, \quad (18)$$

where $\Omega \left(= \frac{\theta - \theta_1}{\theta_0 - \theta_1} \right)$ is determined from equation (14).

$\frac{f}{E\alpha(\theta_1 - \theta_0)}$, determined from equation (18), is a non-dimensional parameter giving the stress distribution in the plate.

4.4 Non-dimensional parameters

An examination of paras. 4.1, 4.2 and 4.3 shows that the basic non-dimensional parameters of the problem are

$$p, q, \frac{hL}{ks} (= \xi), \quad \text{and} \quad \frac{\kappa t}{L^2}.$$

Other non-dimensional parameters

$$\frac{hL^2}{ks}, \quad \frac{\theta - \theta_1}{\theta_0 - \theta_1} (= \Omega), \quad \frac{f}{E\alpha(\theta_1 - \theta_0)},$$

giving the heat transfer coefficient, h , the temperature, θ , and the stress, f , are expressed in terms of p , q , ξ , and $\frac{\kappa t}{L^2}$, in equations (1), (14) and (18).

For $p = 3.5$, $q = 0.1774 \times 10^3$, and $p = 6.5$, $q = 2.506 \times 10^3$, $\frac{hL^2}{ks}$ is plotted against ξ in Fig. 3, and $\frac{\theta - \theta_1}{\theta_0 - \theta_1}$, $\frac{f}{E\alpha(\theta_1 - \theta_0)}$, against ξ for various values of $\frac{\kappa t}{L^2}$ in Figs. 4 and 5. Maximum values of $\frac{f}{E\alpha(\theta_1 - \theta_0)}$ are plotted against $\frac{\kappa t}{L^2}$ in Fig. 6.

5 Numerical examples, relevant to cases of aerodynamic heating in supersonic flight

The theory developed in the preceding section is now used to estimate transient thermal stresses in a plate heated aerodynamically by a supersonic air stream suddenly created over its top surface. The stresses obtained are taken to be indicative of stresses set up in a wing skin - due to chordwise variation of heat transfer coefficient on the wing surfaces - following the sudden acquiring of a high supersonic velocity in actual flight.

A plate of mild steel is considered, heated by an air stream of Mach number 3, (Hoff¹ took a Mach number of 3.1), suddenly created in a lateral direction, over and parallel to the top surface of the plate, as shown in Fig.2(a,b). As in Hoff's example, conditions associated with heating at an altitude of 50,000 feet are assumed. It follows that the stresses obtained correspond to stresses which would be induced in the wing skins of an aircraft if it suddenly acquired a velocity of Mach number 3, at an altitude of 50,000 feet.

The dimensions and physical properties of the plate are given in Table I, together with two sets of values of θ_0 , θ_1 , p , and q , which are chosen to represent, approximately, temperature and heat transfer conditions corresponding to the two different cases of (a) aerodynamic heating with a laminar boundary layer, and (b) aerodynamic heating with a turbulent boundary layer. It is postulated that there is little or no heating before the supersonic air stream is created, so that θ_0 , the initial temperature of the plate, has been equated to the ambient temperature of the air (-70°F at 50,000 feet). θ_1 has been equated to the adiabatic wall temperature of the flow. The assumed heat transfer coefficients (defined by the chosen values of p and q), and the actual heat transfer coefficients derived from Aerodynamics, are plotted together, against ζ , in Fig.3. General expressions for the adiabatic wall temperature, and the heat transfer coefficients derived from Aerodynamics, have been given by Kaye³ - they are summarised, for convenience, in Appendix III.

An outline of the numerical analysis used for determining the transient temperature and stress distributions in the plate is given in Appendix IV.

5.1 Numerical results

Transient temperature and stress distributions, for the two numerical cases considered, are plotted, in non-dimensional form, in Figs. 4(a,b) and 5(a,b). The curves in Fig. 4(a,b) correspond to aerodynamic heating with a laminar boundary layer, while those in Fig.5(a,b) correspond to aerodynamic heating with a turbulent boundary layer.

The main feature of the temperature distributions is a gradient near the leading edge of the plate ($x = 0$), which, from being infinite immediately after the beginning of heat transfer, decreases to zero as the time increases. The occurrence of this gradient is a result of the initial build-up of temperature near the leading edge, caused by the steep rise in heat transfer coefficient as the edge is approached (see Fig.3). The thermal stress distributions across the plate are characterized by two reversals of sign: compressive stresses develop near the edges of the plate, while the middle parts are subjected to tension.

The maximum stress in the plate at various times is plotted, in non-dimensional form, in Fig.6. The stress is located in the region of compression near the leading edge, except for the higher values of time, when it is located at the trailing edge ($x = L$). It assumes its greatest value immediately after the beginning of heat transfer and decreases to zero as the time increases. The decrease in value is much more rapid for heating with a turbulent boundary layer than for heating with a laminar boundary layer - since the plate takes a shorter time to acquire a uniform temperature, with turbulence.

The actual values of the maximum compressive and tensile stresses, and minimum temperatures, at various times after the beginning of heating are given now, below.

(i) For heating with a laminar boundary layer:-

$$-55,800 \frac{\text{lb wt}}{\text{in}^2}, \quad +20,400 \frac{\text{lb wt}}{\text{in}^2}, \quad -16^\circ\text{F}, \quad \text{after 200 secs;}$$

$$-35,900 \frac{\text{lb wt}}{\text{in}^2}, \quad +19,800 \frac{\text{lb wt}}{\text{in}^2}, \quad 57^\circ\text{F}, \quad \text{after 500 secs;}$$

$$-14,500 \frac{\text{lb wt}}{\text{in}^2}, \quad +10,500 \frac{\text{lb wt}}{\text{in}^2}, \quad 235^\circ\text{F}, \quad \text{after 1500 secs;}$$

$$-4,300 \frac{\text{lb wt}}{\text{in}^2}, \quad +2,600 \frac{\text{lb wt}}{\text{in}^2}, \quad 415^\circ\text{F}, \quad \text{after 3500 secs.}$$

(The final temperature throughout the plate is 530°F .)

(ii) For heating with a turbulent boundary layer:-

$$-63,500 \frac{\text{lb wt}}{\text{in}^2}, \quad +22,300 \frac{\text{lb wt}}{\text{in}^2}, \quad 16^\circ\text{F}, \quad \text{after 25 secs;}$$

$$-48,000 \frac{\text{lb wt}}{\text{in}^2}, \quad +20,700 \frac{\text{lb wt}}{\text{in}^2}, \quad 91^\circ\text{F}, \quad \text{after 50 secs;}$$

$$-28,200 \frac{\text{lb wt}}{\text{in}^2}, \quad +16,500 \frac{\text{lb wt}}{\text{in}^2}, \quad 211^\circ\text{F}, \quad \text{after 100 secs;}$$

$$-11,900 \frac{\text{lb wt}}{\text{in}^2}, \quad +9,500 \frac{\text{lb wt}}{\text{in}^2}, \quad 367^\circ\text{F}, \quad \text{after 200 secs;}$$

$$-2,600 \frac{\text{lb wt}}{\text{in}^2}, \quad +2,400 \frac{\text{lb wt}}{\text{in}^2}, \quad 502^\circ\text{F}, \quad \text{after 400 secs.}$$

(The final temperature throughout the plate is 562°F .)

6 Conclusions

It is concluded that, when an aircraft suddenly acquires a high supersonic velocity in flight, it is likely that high transient thermal stresses will be induced in the wing skins, due to chordwise variation of heat transfer coefficient on the wing surfaces.

The analysis shows that:-

- (i) Compressive stresses will develop near the leading and trailing edges, while the middle portions (away from the edges) will be subjected to tension.

- (ii) In general, the maximum stress will occur in the region of compression near the leading edge.
- (iii) For heating with a turbulent boundary layer, the stresses will die away to zero very quickly, but for heating with a laminar boundary layer, they will persist for a considerable time after the attainment of the high supersonic velocity.

The stresses could be reduced by preventing the high build-up of temperature near the leading edge, which it has been shown, accompanies the sudden rise in velocity. This might be effected by applying surface insulation to the leading edge, and by operating a cooling system on the inside surfaces of the wing.

List of Symbols

<u>Symbol</u>	<u>Description</u>	<u>Units</u>
x,y	= distances measured from a point O on one of the longitudinal edges, in lateral and longitudinal directions, respectively.	ft
L	= width of the plate.	ft
s	= thickness of the plate.	ft
k	= thermal conductivity,	$\left. \begin{array}{l} \frac{B \text{ Th } U}{ft^2 (^\circ F/ft) \text{ sec}} \\ \frac{lb}{ft^3} \\ \frac{B \text{ Th } U}{lb \text{ } ^\circ F} \\ \frac{ft^2}{sec} \end{array} \right\} \text{for the material of the plate.}$
ρ	= density,	
c	= specific heat,	
α	= diffusivity = $\frac{k}{\rho c}$,	
t	= time following the beginning of heat transfer between the plate and its surroundings.	sec
$h = h(x)$	= heat transfer coefficient on the top surface of the plate.	$\frac{B \text{ Th } U}{ft^2 \text{ } ^\circ F \text{ sec}}$
Q	= rate of heat transfer across the top surface per unit length of the plate (see equation (2)).	$\frac{B \text{ Th } U}{ft \text{ sec}}$
Q_x	= rate of heat conduction within the plate, parallel to Ox, per unit length of the plate, at x (see equation (3)).	$\frac{B \text{ Th } U}{ft \text{ sec}}$

List of Symbols (Contd)

<u>Symbol</u>	<u>Description</u>	<u>Units</u>
$\theta = \theta(x, t)$	= temperature in the plate (constant through the thickness) at a position x , at time t .	$^{\circ}\text{F}$
θ_0	= initial temperature of the plate and its immediate surroundings.	$^{\circ}\text{F}$
θ_1	= temperature in the immediate proximity of the top surface for $t > 0$ (the final temperature of the plate).	$^{\circ}\text{F}$
$f = f(x, t)$	= longitudinal stress in the plate	$\frac{\text{lb wt}}{\text{in}^2}$
E	= Young's modulus.	$\frac{\text{lb wt}}{\text{in}^2}$
α	= coefficient of linear expansion.	$\frac{\text{in}}{\text{in } ^{\circ}\text{F}}$
p, q	= arbitrary non-dimensional constants such that $p > \frac{1}{2}$, $q > 0$, introduced in equation (1).	
$\left. \begin{array}{l} \frac{x}{L} (= \xi) \\ \frac{kt}{L^2} \end{array} \right\}$	= non-dimensional parameters involving distance x , and time t .	
$\left. \begin{array}{l} \frac{hL^2}{ks} \\ \frac{\theta - \theta_1}{\theta_0 - \theta_1} (= \Omega) \\ \frac{f}{E\alpha(\theta_1 - \theta_0)} \end{array} \right\}$	= non-dimensional parameters given by equations (1), (14) and (18).	
β	= non-dimensional variable of equation (12).	
β_m, β_n	= m^{th} and n^{th} roots (in ascending order of magnitude) of equation (12).	
$X = X(\xi)$	= function of ξ satisfying equation (9).	
η	= independent variable.	
$J_p(\eta)$	= Bessel Function of the First Kind of order p .	
$J'_p(\eta)$	= $\frac{d}{d\eta} [J_p(\eta)]$.	
$I(n, m, p)$	= $\int_0^{\beta n} \eta^m J_p(\eta) d\eta$.	

List of Symbols (Contd)

<u>Symbol</u>	<u>Description</u>
$S_z(\eta)$	$= \int_0^{\eta} \frac{\sin \eta}{\eta} d\eta .$
$\left. \begin{matrix} e_1 \\ a_1 \end{matrix} \right\}$	$=$ constants in equation (16).
A, A_m, A_n	$=$ constant coefficients in equations (11) and (13).
m, n, j	$=$ positive integers.

REFERENCES

<u>No.</u>	<u>Author(s)</u>	<u>Title, etc.</u>
1	N.J. Hoff	Structural Problems of Future Aircraft. Anglo-American Aeronautical Conference, 1951.
2	E.W. Parkes	Transient Thermal Stresses in Wings. Aircraft Engineering, Vol.XXV, No.298, December, 1953.
3	Joseph Kaye	The Transient Temperature Distribution in a Wing Flying at Supersonic Speeds. J. Aero. Sci., Vol.17, December, 1950.
4	F.V. Davies R.J. Monaghan	The Determination of Skin Temperatures Attained in High Speed Flight. C.P.123. February, 1952.
5	T. Norweiller	Rate of Heat Transfer due to Aerodynamic Heating at High Altitudes. RAE Technical Note No. Aero 1834, December, 1946. A.R.C. 10,578.
6	S. Goldstein	Modern Developments in Fluid Dynamics, Vol.II.
7	H.S. Carslaw J.C. Jaeger	Conduction of Heat in Solids.
8	A.E.H. Love	A Treatise on the Mathematical Theory of Elasticity.
9	G.N. Watson	A Treatise on the Theory of Bessel Functions.
10	-	Tables of Spherical Bessel Functions, Vol.I. Mathematical Tables Project, National Bureau of Standards, New York, 1947.
11	-	Tables of Bessel Functions of the First Kind. The Annals of the Computation Laboratory of Harvard University, Vols. III - XIV.

REFERENCES (Contd)

<u>No.</u>	<u>Author(s)</u>	<u>Title, etc.</u>
12	-	British Association Mathematical Tables, Vol.I, Circular and Hyperbolic Functions.
13	-	Tables of Sine and Cosine Integrals. Federal Works Agency, New York, 1942.
14	E. Jahnke F. Emde	Tables of Functions.

APPENDIX I

Determination of the coefficients, A_n

Lommel Integrals⁹, deduced from Bessel's Equation, are

$$\left. \begin{aligned} \int_0^1 \xi J_p(\beta_n \xi) J_p(\beta_m \xi) d\xi &= \frac{1}{\beta_n^2 - \beta_m^2} \left[\beta_m J_p(\beta_n) J_p'(\beta_m) - \beta_n J_p(\beta_m) J_p'(\beta_n) \right], \\ \int_0^1 \xi [J_p(\beta_n \xi)]^2 d\xi &= \frac{1}{2\beta_n^2} \left[\beta_n^2 [J_p'(\beta_n)]^2 + (\beta_n^2 - p^2) [J_p(\beta_n)]^2 \right]. \end{aligned} \right\} (19)$$

Now equation (12) may be written in the form

$$J_p(\beta) + 2\beta J_p'(\beta) = 0, \quad (20)$$

so that if β_n, β_m are different roots of equation (12), then

$$\left. \begin{aligned} J_p(\beta_n) + 2\beta_n J_p'(\beta_n) &= 0, \\ J_p(\beta_m) + 2\beta_m J_p'(\beta_m) &= 0. \end{aligned} \right\} (21)$$

Combining equations (19) and (21) yields

$$\left. \begin{aligned} \int_0^1 \xi J_p(\beta_n \xi) J_p(\beta_m \xi) d\xi &= 0, \\ \int_0^1 \xi [J_p(\beta_n \xi)]^2 d\xi &= \frac{1}{2\beta_n^2} (4 - p^2 + \beta_n^2) [J_p(\beta_n)]^2. \end{aligned} \right\} (22)$$

The constant coefficients A_n in equation (13) may now be determined. Equation (13) must satisfy the initial condition that $\theta = \theta_0$ at $t = 0$, and, therefore,

$$\theta_0 - \theta_1 = \sum_{n=1}^{\infty} A_n \xi^{\frac{1}{2}} J_p(\beta_n \xi). \quad (23)$$

Multiplying both sides of equation (23) by $\xi^{\frac{1}{2}} J_p(\beta_n \xi)$ and then integrating between 0 and 1, using equations (22), gives

$$\begin{aligned}
 A_n &= (\theta_0 - \theta_1) \frac{\int_0^1 \xi^{\frac{1}{2}} J_p(\beta_n \xi) d\xi}{\int_0^1 \xi [J_p(\beta_n \xi)]^2 d\xi} \\
 &= \frac{2(\theta_0 - \theta_1) \beta_n^{\frac{1}{2}}}{(1 - p^2 + \beta_n^2) [J_p(\beta_n)]^2} \int_0^{\beta_n} \eta^{\frac{1}{2}} J_p(\eta) d\eta.
 \end{aligned}
 \tag{24}$$

Substituting this expression for A_n into equation (13) yields equation (14).

APPENDIX II

Derivation of expressions for $I(n, \frac{1}{2}, p)$, $p = \frac{2j+1}{2}$ ($j = 1, 2, \dots, 6$)

Taking

$$I(n, m, p) = \int_0^{\beta_n} \eta^m J_p(\eta) d\eta, \quad (25)$$

integration by parts leads to the recurrence relation

$$I(n, m, p) = \frac{\beta_n^{m+1} J_p(\beta_n)}{m-p+1} - \frac{I(n, m+1, p-1)}{m-p+1}, \quad (26)$$

which may be used providing that $m+p+1 > 0$, $m-p+1 \neq 0$, $m+1 \neq 0$. Using the relation, the integrals $I(n, \frac{1}{2}, p)$ $p = \frac{2j+1}{2}$ ($j = 2, \dots, 6$), may be determined in terms of the integrals

$$\begin{aligned} & I\left(n, \frac{3}{2}, \frac{5}{2}\right), \quad I\left(n, \frac{5}{2}, \frac{7}{2}\right), \\ & I\left(n, \frac{3}{2}, \frac{3}{2}\right), \quad I\left(n, \frac{5}{2}, \frac{5}{2}\right), \quad I\left(n, \frac{7}{2}, \frac{7}{2}\right), \end{aligned}$$

as follows:

$$\left. \begin{aligned} I\left(n, \frac{1}{2}, \frac{5}{2}\right) &= -\beta_n^{3/2} J_{5/2}(\beta_n) + I\left(n, \frac{3}{2}, \frac{3}{2}\right), \\ I\left(n, \frac{1}{2}, \frac{7}{2}\right) &= -\frac{1}{2} \beta_n^{3/2} J_{7/2}(\beta_n) + \frac{1}{2} I\left(n, \frac{3}{2}, \frac{5}{2}\right), \\ I\left(n, \frac{1}{2}, \frac{9}{2}\right) &= -\frac{1}{3} \beta_n^{3/2} \left[J_{9/2}(\beta_n) + \beta_n J_{7/2}(\beta_n) \right] + \frac{1}{3} I\left(n, \frac{5}{2}, \frac{5}{2}\right), \\ I\left(n, \frac{1}{2}, \frac{11}{2}\right) &= -\frac{1}{4} \beta_n^{3/2} \left[J_{11/2}(\beta_n) + \frac{1}{2} \beta_n J_{9/2}(\beta_n) \right] + \frac{1}{8} I\left(n, \frac{5}{2}, \frac{7}{2}\right), \\ I\left(n, \frac{1}{2}, \frac{13}{2}\right) &= -\frac{1}{5} \beta_n^{3/2} \left[J_{13/2}(\beta_n) + \frac{1}{3} \beta_n J_{11/2}(\beta_n) + \frac{1}{3} \beta_n^2 J_{9/2}(\beta_n) \right] \\ &\quad + \frac{1}{15} I\left(n, \frac{7}{2}, \frac{7}{2}\right). \end{aligned} \right\} (27)$$

Now starting with the relations

$$\sqrt{\frac{\pi}{2}} \eta^{\frac{1}{2}} J_{\frac{1}{2}}(\eta) = \sin \eta, \quad \sqrt{\frac{\pi}{2}} \eta^{\frac{1}{2}} J_{\frac{3}{2}}(\eta) = \cos \eta, \quad (28)$$

and using the recurrence relation

$$J_{p+1}(\eta) = \frac{2p}{\eta} J_p(\eta) - J_{p-1}(\eta), \quad (29)$$

it may be shown that

$$\left. \begin{aligned} \sqrt{\frac{\pi}{2}} \cdot \eta^{3/2} J_{3/2}(\eta) &= \sin \eta - \eta \cos \eta, \\ \sqrt{\frac{\pi}{2}} \cdot \eta^{5/2} J_{5/2}(\eta) &= (3 - \eta^2) \sin \eta - 3\eta \cos \eta, \\ \sqrt{\frac{\pi}{2}} \cdot \eta^{7/2} J_{7/2}(\eta) &= (15 - 6\eta^2) \sin \eta - (15\eta - \eta^3) \cos \eta. \end{aligned} \right\} \quad (30)$$

By integrating these equations (30) it may be further shown that

$$\left. \begin{aligned} I\left(n, \frac{1}{2}, \frac{3}{2}\right) &= \sqrt{\frac{2}{\pi}} [\text{Si}(\beta_n) - \sin \beta_n], \\ I\left(n, \frac{3}{2}, \frac{5}{2}\right) &= \sqrt{\frac{2}{\pi}} [3 \text{Si}(\beta_n) - 4 \sin \beta_n + \beta_n \cos \beta_n], \\ I\left(n, \frac{5}{2}, \frac{7}{2}\right) &= \sqrt{\frac{2}{\pi}} [15 \text{Si}(\beta_n) + (\beta_n^2 - 23) \sin \beta_n + 8\beta_n \cos \beta_n], \\ I\left(n, \frac{3}{2}, \frac{3}{2}\right) &= \sqrt{\frac{2}{\pi}} [-\beta_n \sin \beta_n + 2(1 - \cos \beta_n)], \\ I\left(n, \frac{5}{2}, \frac{5}{2}\right) &= \sqrt{\frac{2}{\pi}} [-5\beta_n \sin \beta_n + (\beta_n^2 - 8) \cos \beta_n + 8], \\ I\left(n, \frac{7}{2}, \frac{7}{2}\right) &= \sqrt{\frac{2}{\pi}} [\beta_n(\beta_n^2 - 33) \sin \beta_n + (9\beta_n^2 - 48) \cos \beta_n + 48]. \end{aligned} \right\} \quad (31)$$

Thus, equations (27) and (31), when taken together, give

$$I\left(n, \frac{1}{2}, p\right), \quad p = \frac{2j+1}{2} \quad (j = 1, 2, \dots, 6),$$

in terms of powers of

$$\beta_n, J_p(\beta_n), \frac{\sin}{\cos} \beta_n, \text{ and } \text{Si}(\beta_n).$$

APPENDIX III

Heat transfer data for a flat plate

Expressions giving the adiabatic wall temperature and surface heat transfer coefficients, for supersonic air flow over a flat plate, have been summarised by Kaye¹. They are now presented, with a numerical application relevant to the examples considered in the main body of the Report.

The following symbols, denoting physical properties of the air, are used:

V = velocity of the air stream over the plate,

V_s = speed of sound in the free stream conditions,

M = Mach number of the flow

$$= \frac{V}{V_s},$$

k' = thermal conductivity,

ρ' = density,

c'_p, c'_v = specific heats at constant pressure and constant volume,

μ = viscosity,

σ = Prandtl number

$$= \frac{c'_p \mu}{k'},$$

Re_L = Reynolds number

$$= \frac{\rho' VL}{\mu}$$

$$\gamma = \frac{c'_p}{c'_v}$$

θ_a = ambient or free stream temperature ($^{\circ}\text{F Abs.}$),

θ_s = stagnation temperature ($^{\circ}\text{F Abs.}$),

θ_w = adiabatic wall temperature ($^{\circ}\text{F Abs.}$),

r = recovery factor

$$= \frac{\theta_w - \theta_a}{\theta_s - \theta_a}.$$

The adiabatic wall temperature is given by

$$\theta_w = \theta_a \left(1 + \frac{1}{2} r (\gamma - 1) M^2 \right), \quad (32)$$

where

$$\left. \begin{aligned} r &= \sigma^{1/2}, \text{ for a laminar boundary layer,} \\ &= \sigma^{1/3}, \text{ for a turbulent boundary layer.} \end{aligned} \right\} (33)$$

Heat transfer coefficients are given by

$$\left. \begin{aligned} \frac{h}{c_p^t \rho^t V} &= \frac{0.330}{\xi^{1/2} Re_L^{1/2} \sigma^{2/3}}, \text{ for a laminar boundary layer,} \\ &= \frac{0.030}{\xi^{1/5} Re_L^{1/5} \sigma^{2/3}}, \text{ for a turbulent boundary layer.} \end{aligned} \right\} (34)$$

Using equations (32), (33) and (34), θ_w and $\frac{h}{c_p^t \rho^t V}$ are now evaluated for the aerodynamic heating of a plate by an air stream of Mach number 3, in conditions corresponding to an altitude of 50,000 feet.

For ambient air at an altitude of 50,000 feet (at a temperature of -70°F):

$$\begin{aligned} k^t &= 3.12 \times 10^{-6} \frac{\text{B Th U}}{\text{ft}^2 \left(\frac{^\circ\text{F}}{\text{ft}} \right) \text{sec}}, & c_p^t &= 0.240 \frac{\text{B Th U}}{\text{lb } ^\circ\text{F}}, \\ \rho^t &= 0.01169 \frac{\text{lb}}{\text{ft}^3}, & V_s &= 968 \frac{\text{ft}}{\text{sec}}, \\ \sigma &= 0.730, & \gamma &= 1.40. \end{aligned}$$

Using these values, it follows that, for a laminar boundary layer,

$$\begin{aligned} \theta_w &= 530^\circ\text{F}, \\ \frac{h}{c_p^t \rho^t V} &= \frac{0.03134 \times 10^{-3}}{\xi^2}, \end{aligned}$$

and for a turbulent boundary layer,

$$\begin{aligned} \theta_w &= 562^\circ\text{F}, \\ \frac{h}{c_p^t \rho^t V} &= \frac{1.226 \times 10^{-3}}{\xi^{1/5}}. \end{aligned}$$

Kaye has pointed out that the above procedure of evaluating the properties of the air at ambient conditions, for use in equations (32), (33) and (34), is open to some doubt.

APPENDIX IV

Numerical analysis

An outline of the numerical analysis, used for determining the transient temperature and stress distributions in the plate, is now given.

The procedure consists of evaluating:

- (i) the first few roots of equation (12);
- (ii) the integral $I(n, \frac{1}{2}, p) = \int_0^{\beta_n} \eta^{\frac{1}{2}} J_p(\eta) d\eta$, for each root;
- (iii) the sum of the first few terms of the series in equation (14) (each term corresponding to an evaluated root), yielding an approximate value of $\frac{\theta - \theta_1}{\theta_0 - \theta_1}$; for various values of ξ and t ;
- (iv) the integrals $\int_0^1 \Omega d\xi$ and $\int_0^1 \xi \Omega d\xi$, which facilitate the evaluation of $\frac{\partial(\theta_1 - \theta_0)}{\partial t}$, using equation (18).

The numerical work is simplified when p is an integer or half-integer, since tabulated values of Bessel Functions^{10, 11, 14} may then be used in the computations.

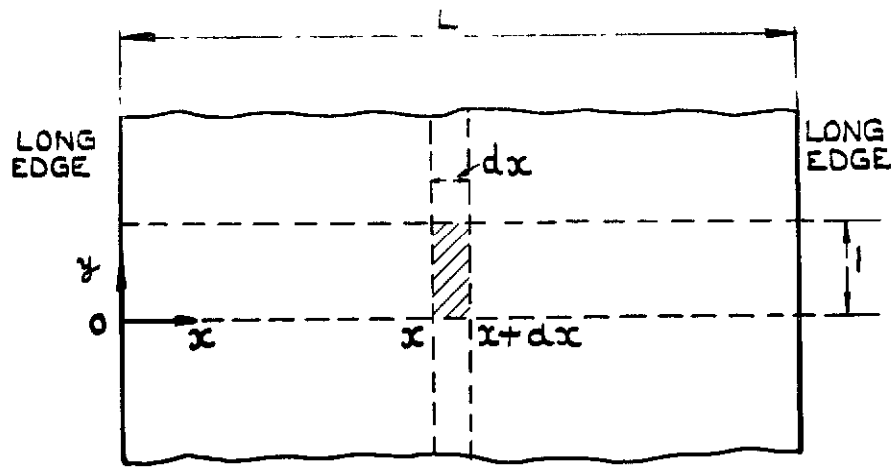
In the two numerical cases considered (corresponding to $p = 3.5$ and 6.5 , respectively), the first 13 roots of equation (12) were determined. For $p = 3.5$, the integrals $I(n, \frac{1}{2}, \frac{7}{2})$, $n = 1, 2, \dots, 13$, were evaluated using expressions derived in Appendix II, while for $p = 6.5$, the integrals $I(n, \frac{1}{2}, \frac{13}{2})$, $n = 1, 2, \dots, 13$, were evaluated using numerical methods of integration. Values of $\frac{\theta - \theta_1}{\theta_0 - \theta_1}$ ($= \Omega$), obtained by using equation (14) in matrix form, were found to be inaccurate for the smaller values of ξ and t . (The ranges of inaccuracy correspond to the dotted parts of the curves in Figs. 4(a) and 5(a).) Greater accuracy could have been obtained by taking more roots of equation (12), but this was considered unnecessary.

The integrals $\int_0^1 \Omega d\xi$ and $\int_0^1 \xi \Omega d\xi$, were determined graphically from plotted values of Ω and $\xi \Omega$.

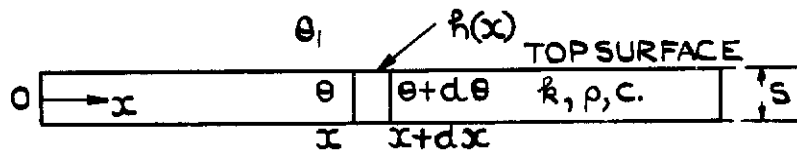
TABLE I

Data for the Numerical Examples

	Symbol	Numerical Value	Units
Dimensions of the plate cross-section.	L	7	ft
	s	3/8	in
Physical constants for the plate.	k	7.20×10^{-3}	B Th U/ft ² ($\frac{^{\circ}\text{F}}{\text{ft}}$) sec
	ρ	490	lb/ft ³
	c	0.120	B Th U/lb $^{\circ}\text{F}$
	κ	0.1224×10^{-5}	ft ² /sec
	E	29×10^6	lbs wt/in ²
	α	6.5×10^{-6}	in/in $^{\circ}\text{F}$
Aerodynamic heating with a laminar boundary layer on the plate.	θ_0	-70	$^{\circ}\text{F}$
	θ_1	530	$^{\circ}\text{F}$
	p	3.5	-
	q	0.1774×10^3	-
	$\frac{1}{10^3} \cdot \frac{hL^2}{ks} = \frac{1}{10^3} \left(\frac{p^2 - \frac{1}{4}}{\xi^2} + q \right)$	$\frac{0.012}{\xi^2} + 0.1774$	-
Aerodynamic heating with a turbulent boundary layer on the plate.	θ_0	-70	$^{\circ}\text{F}$
	θ_1	562	$^{\circ}\text{F}$
	p	6.5	-
	q	2.306×10^3	-
	$\frac{1}{10^3} \cdot \frac{hL^2}{ks} = \frac{1}{10^3} \left(\frac{p^2 - \frac{1}{4}}{\xi^2} + q \right)$	$\frac{0.042}{\xi^2} + 2.306$	-

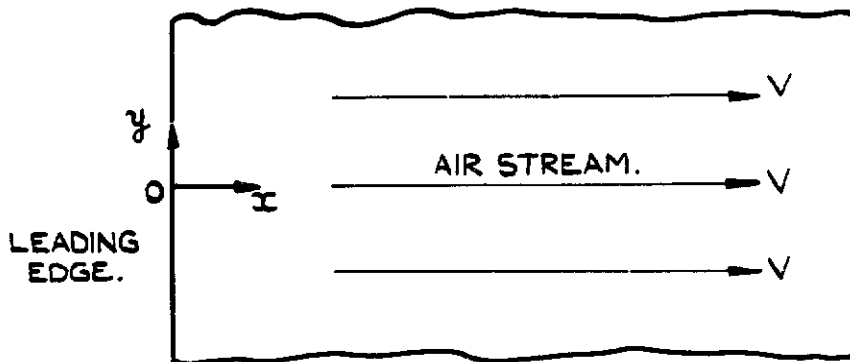


(a) PLAN

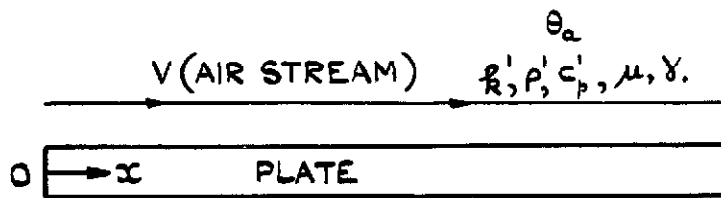


(b) LATERAL CROSS-SECTION.

FIG. 1(a&b) THE PLATE, SHOWING NOTATION.



(a) PLAN



(b) LATERAL CROSS-SECTION

FIG. 2(a&b) AERODYNAMIC HEATING OF THE PLATE, SHOWING THE DIRECTION OF THE SUPERSONIC AIR STREAM OVER THE TOP SURFACE.

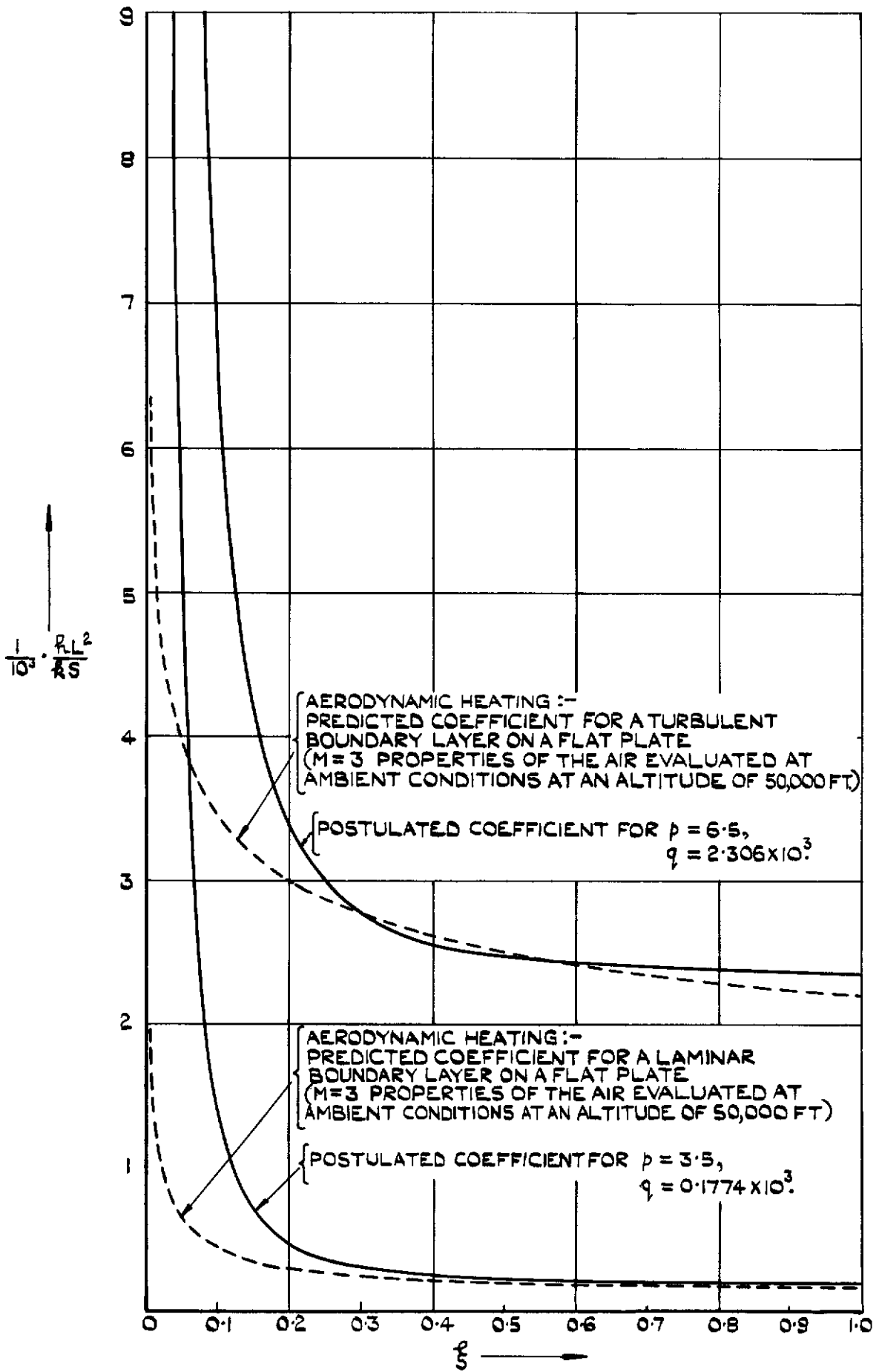
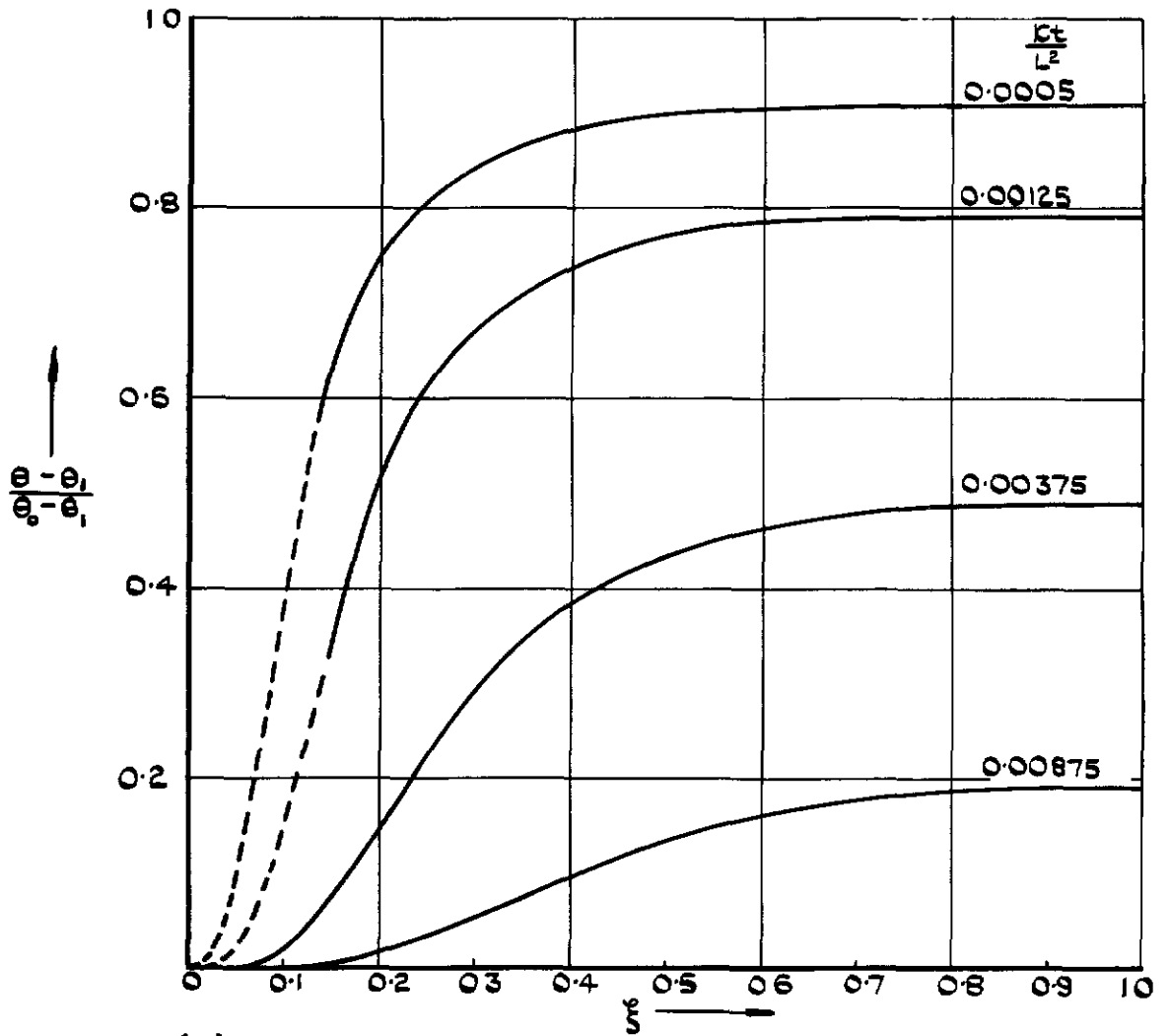
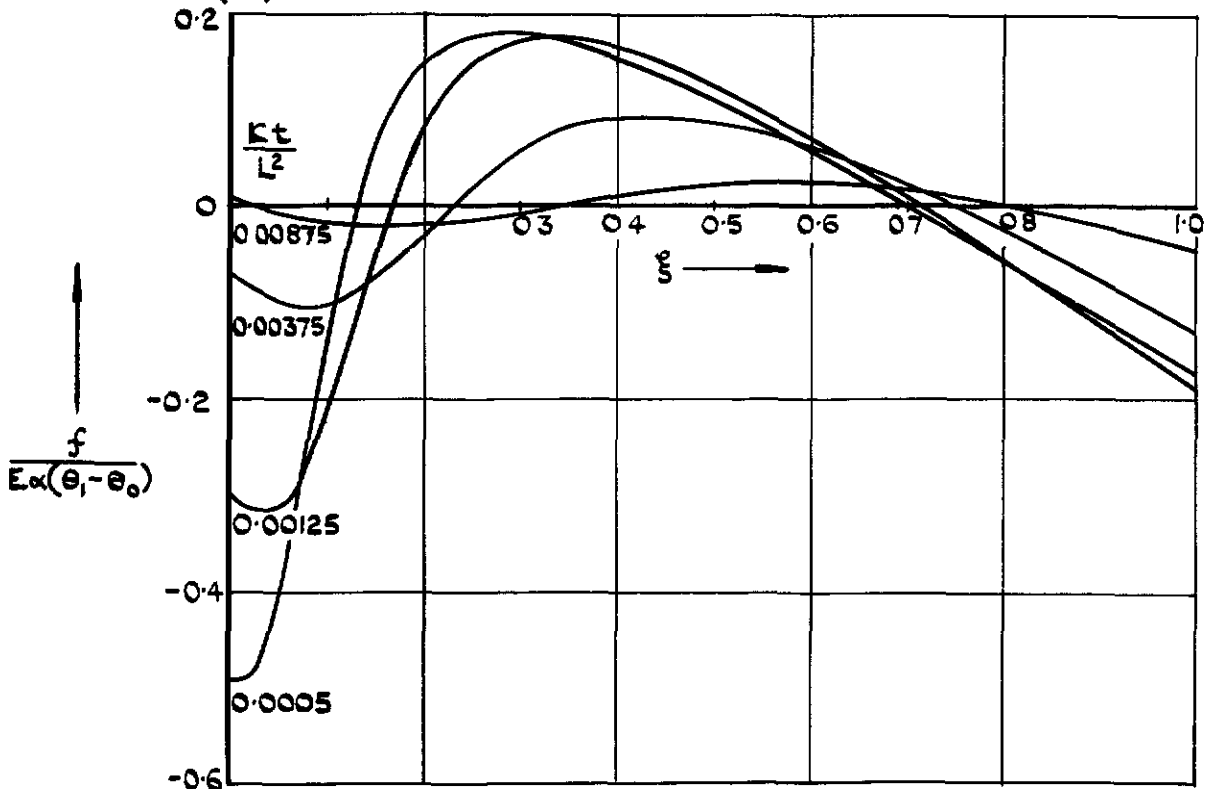


FIG.3. HEAT TRANSFER COEFFICIENTS.

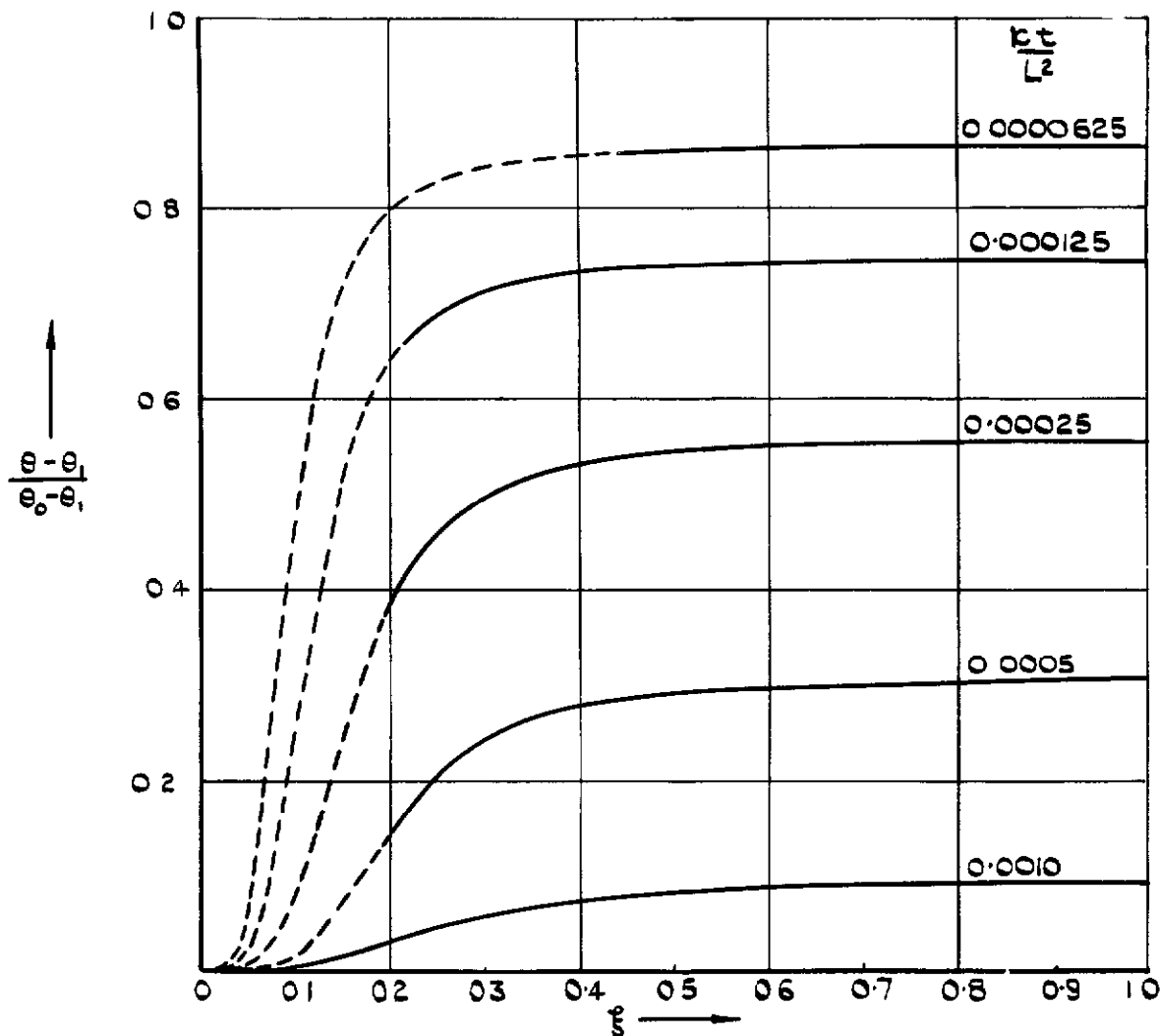


(a) TEMPERATURE DISTRIBUTION.

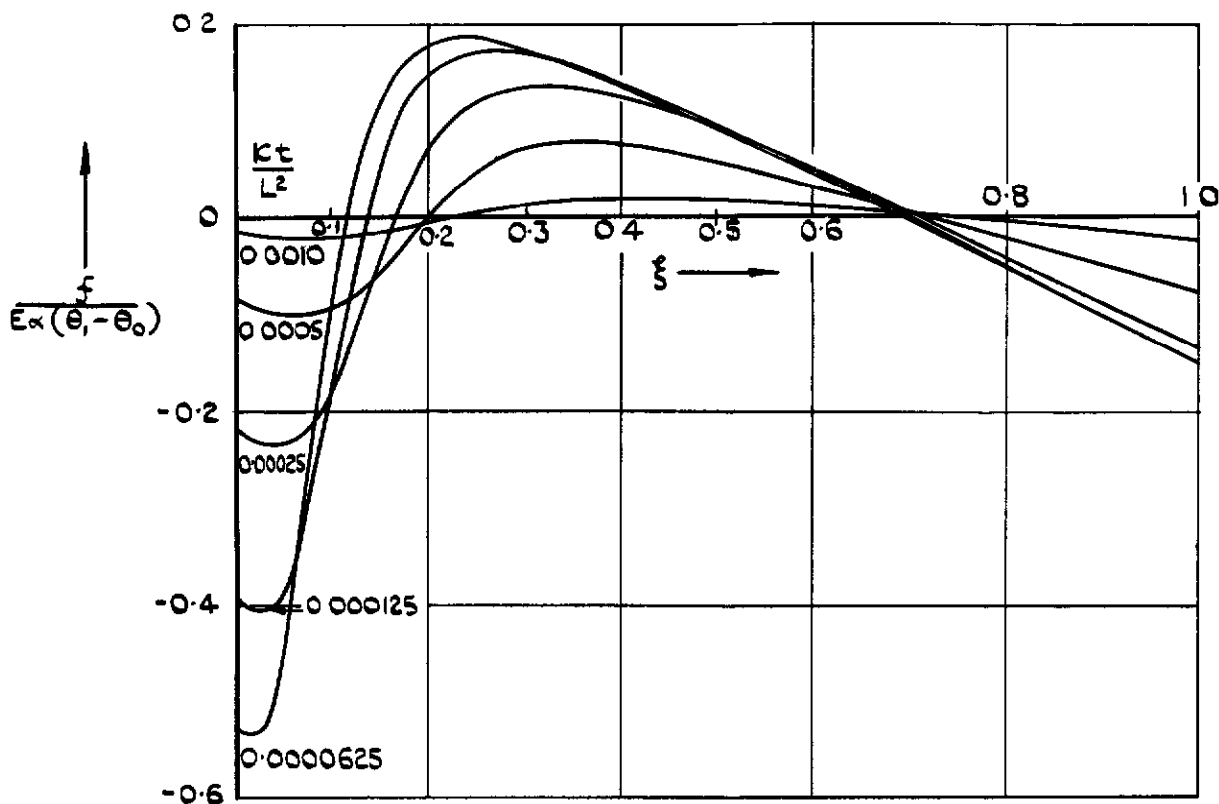


(b) STRESS DISTRIBUTION.

FIG.4(a&b) TEMPERATURE AND STRESS DISTRIBUTIONS IN THE PLATE AT VARIOUS TIMES FOR $\frac{1}{10^3} \cdot \frac{\rho L^2}{kS} = \frac{0.012}{\xi^2} + 0.1774$ ($P = 3.5$, $q = 0.1774 \times 10^3$), THE NUMBERS ON THE CURVES ARE VALUES OF kt/L^2 (CORRESPONDING TO $\tau = 200, 500, 1500, 3500$ SECS. FOR THE PLATE TAKEN AS EXAMPLE). THE RESULTS ARE ASSOCIATED WITH AERODYNAMIC HEATING WITH A LAMINAR BOUNDARY LAYER.



(a) TEMPERATURE DISTRIBUTION.



(b) STRESS DISTRIBUTION.

FIG. 5 (a&b) TEMPERATURE AND STRESS DISTRIBUTIONS IN THE PLATE AT VARIOUS TIMES FOR $\frac{1}{10^3} \cdot \frac{kL^2}{\rho S} = \frac{0.042}{\xi^2} + 2.306$ ($\rho = 6.5, q = 2.306 \times 10^3$). THE NUMBERS ON THE CURVES ARE VALUES OF kt/L^2 (CORRESPONDING TO $t = 25, 50, 100, 200, 400$ SECS. FOR THE PLATE TAKEN AS EXAMPLE). THE RESULTS ARE ASSOCIATED WITH AERODYNAMIC HEATING WITH A TURBULENT BOUNDARY LAYER.

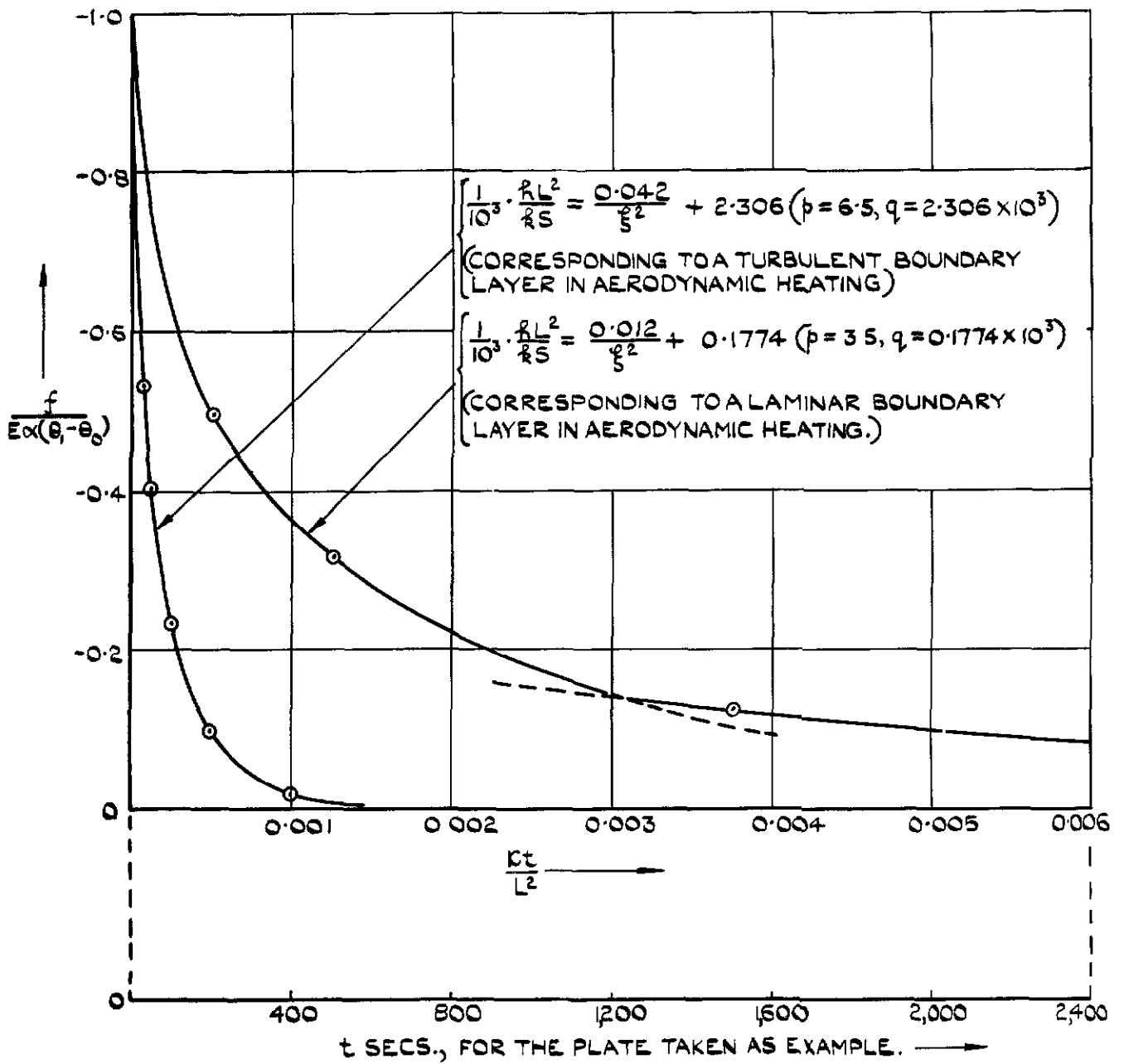


FIG. 6 MAXIMUM STRESS IN THE PLATE AT VARIOUS TIMES.

THE CURVES ARE BASED ON VALUES OBTAINED FROM FIG. 4. AND FIG. 5, AS SHOWN.

C.P. No. 299

(16,932)

A.R.C. Technical Report

Crown copyright reserved

Published by

HER MAJESTY'S STATIONERY OFFICE

To be purchased from

York House, Kingsway, London W C 2

423 Oxford Street, London W 1

P O Box 569, London S E 1

13A Castle Street, Edinburgh 2

109 St Mary Street, Cardiff

39 King Street, Manchester 2

Tower Lane, Bristol 1

2 Edmund Street, Birmingham 3

80 Chichester Street, Belfast

or through any bookseller

PRINTED IN GREAT BRITAIN

S.O. Code No. 23-9009-99

C.P. No. 299